International Journal of Latest Engineering Research and Applications (IJLERA) ISSN: 2455-7137

Volume – 11, Issue – 10, October 2026, PP – 21-29

Effect of Magnesium and Copper Additions on the Mechanical Properties and Microstructure of Recycled Aluminum Castings

Ali Jasim Atiyah[1], Raed Salman Saeed[1], Alaa Shaker Obaida[1]*

[1]*Al-Furat Al-Awsat Technical University, Iraq*

**Corresponding Author*

ORCID: Ali Jasim Atiyah: 0009-0008-2357-7749 | Raed Salman Saeed: 0009-0003-5756-7139

Alaa Shaker Obaida: 0009-0006-0170-3404

Abstract: This study investigates the mechanical properties, creep response, porosity, and microstructural characteristics of recycled aluminum beverage-can castings modified through simultaneous magnesium and copper additions. Four compositions (S1–S4) were prepared by gravity casting into a steel mold preheated to 300°C, with a pouring temperature of 750°C. Nominal additions ranged from 0 to 3 wt.% Mg and from 0 to 1.5 wt.% Cu. Bulk elemental composition was assessed by optical emission spectroscopy, while tensile strength, elongation, Vickers hardness, and tensile creep behavior were evaluated experimentally. Creep tests were conducted at 200°C under a constant 2.5 kN tensile load for 3600 s. Porosity was assessed using immersion-based density measurements, and selected specimens were examined using scanning electron microscopy and energy-dispersive X-ray spectroscopy. The study compares measured responses across the four compositions and examines associations between overall alloy chemistry, casting porosity, and mechanical behavior. Because manganese also varied across the compositions, the experimental design does not isolate the individual contributions of magnesium and copper. Phase identification and quantitative grain-size measurements were outside the scope of the investigation.

Keywords: Aluminum recycling, Copper additions, Creep behavior, Gravity casting, Magnesium additions, Mechanical properties, Microstructure, Optical emission spectroscopy, Porosity, Scanning electron microscopy

1. Introduction

Aluminium is one of the most common engineering materials in the present industries due to its extraordinary properties such as low density (almost 2.7 g/cm3), high thermal and electrical conductivity, high corrosion resistant rate forming its protective oxide layer. Moreover, it has a high strength-weight ratio and is hence suitable especially in lightweight structure applications. To enhance the mechanical properties, it is typically alloyed with others such as Magnesium (Mg) and Copper (Cu) [1,2]. These alloying elements are important to alter the microstructure and enhance deformation resistance by solid solution hardening and precipitation hardening[3]. Aluminium recycling is thus an important sustainable industrial practice, as it can reduce the primary aluminium production energy requirements by as much as 95% [20].

But multiple remelting operations may have adverse impacts on microstructure and mechanical properties of aluminum. Aluminium is a highly oxidizable material and on melting it produces aluminium oxide (Al2O3) which can be trapped in the melt as non-metallic inclusions, which affect the quality of the casting. In addition, molten aluminum is extremely susceptible to the presence of hydrogen, which can lead to gas porosity during solidification, significantly affecting mechanical properties like strength and hardness. [6,7] Mechanical behavior of aluminum alloys is strongly affected by microstructural features; grain size, phase distribution and content of defects. The Hall–Petch equation states that the increase in strength can be attributed to the increase of the number of grain boundaries that hinder dislocation motion in the material [9,10]. The mechanical properties and microstructural features of aluminum alloys can be altered by adding alloying elements like Mg and Cu, which can be accomplished by the solid solution strengthening of alloys and the alteration of the distribution of secondary constituents [11,12,17]. In the present study, however, a quantitative grain refinement and the formation of certain intermetallic phases have not been independently established. [13]

The recycled aluminum material and the influence of each alloying element have been targeted by previous studies. In this work, the simultaneous additions of Mg and Cu and the resulting changes in the combined composition are investigated in the Al of a beverage can on a consistent gravity casting basis. As a result of the varying of Mg and Cu and the varying of Mn between compositions, the individual causal contributions and any synergy was not separated from this experimental design. Four as-cast compositions are compared using bulk OES, tensile testing, Vickers hardness, creep testing, recorded porosity and SEM/EDS.

 2026 IJLERA – All Right Reserved

The investigation is based on gravity casting in a steel mold preheated to 300°C with natural cooling in the mold in ambient laboratory conditions. These casting and testing conditions are only those used in this experiment and should not necessarily be considered optimal in other applications of a different alloy.

2. Materials and Methodology

2.1 Materials

The main raw material used to make the castings of recycled Al was post-consumer Al beverage cans. The powders were used to provide the alloying additions and were magnesium (Mg) and copper (Cu) with nominal purities of about 99% and particle sizes of about 50 µm, respectively. The four compositions studied were: recycled aluminum (S1); recycled aluminum + 1 wt.% Mg and 0.5wt.% Cu (S2); recycled aluminum + 2 wt.% Mg and 1wt.% Cu (S3); recycled aluminum + 3 wt.% Mg and 1.5wt.% Cu (S4). The percent additions are nominal and not the actual measured alloy composition. In Table 1 the materials used are summarized.

Table 1: Materials used in this study

Material	Form / Source	Purity (%)	Particle Size	Composition / Amount
Recycled Aluminum	Beverage cans	—	—	Base material
Magnesium (Mg)	Powder	~99	~50 µm	1–3 wt.%
Copper (Cu)	Powder	~99	~50 µm	0.5–1.5 wt.%

The recycled aluminium was sourced from post-consumer beverage cans that can vary in the aluminium alloy series used in the body, lids and pull tabs. The remelted base material was thus processed as a mixed recycled Al alloy. The chemical composition of alloys S1, S2, S3 and S4 were measured experimentally by optical emission spectroscopy (OES) instead of being estimated for the individual can components.

2.1.1 Bulk Chemical Composition Analysis

Bulk compositions were measured using a SPECTROMAXx LMX09 optical emission spectrometer (Germany) following ASTM E1251. In each composition, one OES measurement was taken on the as-cast surface of a specimen that was polished. No information was available about the calibration of any of the instruments, nor could the repeatability of the measurements within the same composition be assessed. The reported values are thus a single bulk OES measurement for each composition (Table 2).

Table 2: Chemical composition of the recycled aluminum samples determined by OES (wt.%)

Element (wt.%)	S1	S2	S3	S4
Al	96.82	95.67	93.73	91.81
Mn	1.00	0.70	1.20	1.70
Mg	1.30	2.30	3.10	4.40
Fe	0.48	0.42	0.50	0.28
Si	0.25	0.18	0.22	0.12
Cu	0.02	0.63	1.10	1.60
Zn	0.10	0.02	0.08	0.03
Ti	0.03	0.02	0.03	0.02
Cr	0.00	0.06	0.04	0.04
Total	100.00	100.00	100.00	100.00

2.2 Melting and Casting Procedure

The recycled Al beverage cans were melted at the temperature range of 720-750°C and the approximate particle size was about 50 µm. The Mg and Cu powders were mixed and wrapped in Al foil, and poured simultaneously as a part of the molten Al according to the nominal compositions. The stirring time was about 3-5 minutes and the holding time was about 3 minutes in the melt before the pouring. Floating slag and surface oxides were manually removed before pouring. No fluxing, degassing in inert gas or chemical degassing treatment was applied. The molten alloy was poured at a temperature of 750°C into a permanent steel mold, preheated to 300°C. The castings were left to cool down in the mould in ambient laboratory conditions. Each composition was cast independently four times.

 2026 IJLERA – All Right Reserved

Table 3: Nominal compositions of the investigated recycled aluminum alloys.

Samples	**Composition**
S1	Recycled aluminum(without additives)
S2	Al + 1% Mg + 0.5% Cu
S3	Al + 2% Mg + 1% Cu
S4	Al + 3% Mg + 1.5% Cu



Fig. 2: Schematic representation of the permanent steel mold used for gravity casting. The mold length was 180 mm, while the final cast aluminum ingot was approximately 150 mm long.

3. Samples Tests

3.1 Tensile Test

The prepared samples were subjected to tensile tests to evaluate the mechanical properties of the prepared samples.The cast ingots were machined into standard round tensile test specimens using ASTM E8/E8M. The specimens were of the standard proportional geometry (G ~ 4D), with gauge length (G) of 50 mm, gauge diameter (D) of 12.5 mm and fillet radius (R) of 10 mm.

Tensile tests were performed at room temperature in an Instron 5982 universal testing machine in accordance with the procedure of ASTM E8/E8M. This was not direct strain-rate control, but rather, a fixed crosshead displacement speed of 4.5 mm/min. Four separate specimens of each composition were cast for testing. Ultimate tensile strength and elongation was measured.

3.2 Creep Test

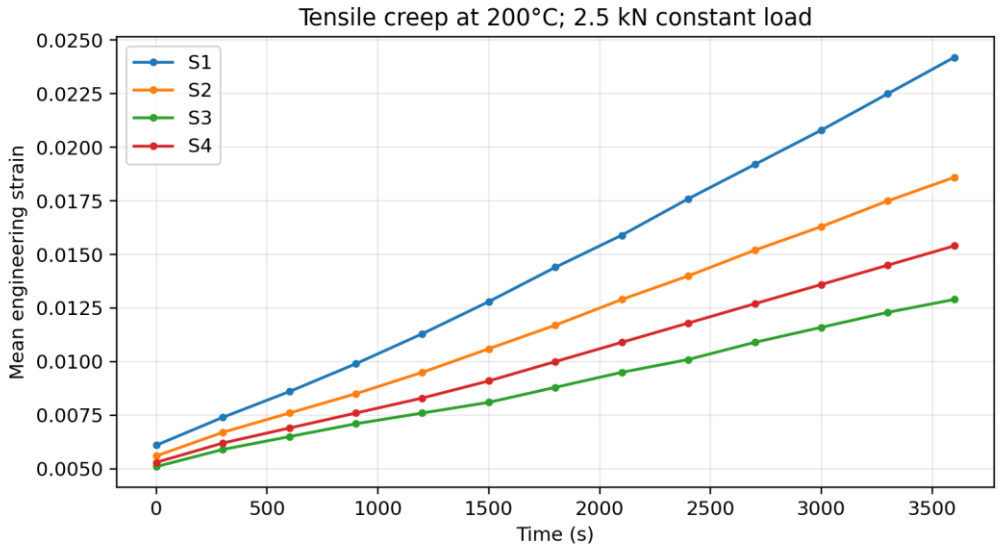
Tensile creep testing was done in an ATS lever arm creep testing machine based on ASTM E139 test reference. The obtained subjects were milled and surface grinding process was carried out and flat rectangular specimens were obtained. The gauge length, width and thickness of their gauge were 25 mm, 10 mm and 5 mm, respectively, and thus, the initial cross section of the gauge was 50 mm². A 2.5kN load was subjected to constant applied tensile load (initially nominal tensile stress 50MPa). Directly attached to the specimen to measure the specimen temperature was a thermocouple. This load was applied only after the samples were thermally stabilized at 200°C and there was no fixed soaking time. Tests lasted 3600 s. The machine was programmed to record the displacement, and to automatically correct the machine for compliance, and calculate the engineering

 2026 IJLERA – All Right Reserved

strain from the corrected displacement and the original 25 mm gauge length. For each alloy composition, four independent creep tests were performed and a total of 16 tests were performed (n = 4). Strain–time data reported is the mean of four specimens at each composition.

The strain–time data for this revision are the average for four creep specimens of each composition over a period of 3600 s, sampled at intervals of 300 s. The automatically calculated creep rates are included in the table below and are shown in Table 4. The interval of the rate and specimen traces for the software-derived rate uncertainty could not be obtained for verification of independence. Note that the rates given are descriptive only and do not claim a specific fitting window with zero steady state.

Supplementary Fig. S1. Average creep strain-time curves of S1–S4 (average of 4 independently cast specimens for each composition). There was no information provided on individual-specimen traces and uncertainty bands.



3.3 Hardness Test

Hardness was measured as Vickers hardness, which was done on a Wilson VH3100 tester, according to ASTM E384. The test force was 500 gf (HV0.5), and dwell time 12 s. The hardness was measured in four independent specimens for each composition; three indentations were taken on each specimen (a total of 12 indentation readings for each composition). The reported hardness standard deviations provide only a summary of the 12 indentation hardness readings, not a comparison of the four specimen level means; original individual indentation hardness readings were not available to recalculate.

3.4 Porosity Analysis

An analytical balance (Mettler Toledo XS204) was used to measure the experimental density via the Archimedes method. There were four independent samples per composition (N = 16). They were all weighed in air and then directly placed in water without coating. The apparent immersed mass was measured after the removal of any adhering air bubbles. The theoretical densities were calculated based on the OES compositions by the rule of mixtures. The conformance in accordance with a particular density-testing standard is not claimed.

$$\rho_{\text{measured}} = \frac{m_{\text{air}}}{m_{\text{air}} - m_{\text{immersed}}} \times \rho_{\text{water}}$$

where m_air is the specimen mass measured in air, m_immersed is its apparent mass during immersion in water, and ρ_water is the density of water.

$$\rho th = 1 / \Sigma(wi/\rho i)$$

where wi is the mass fraction and ρi is the density of each element in the mixture. The theoretical densities were calculated as 2.707, 2.698, 2.705, and 2.699 g/cm³, for S1, S2, S3, and S4, respectively. The percentage of porosity was then determined from:

$$\text{Porosity } (\%) = [1 - (\rho\text{measured} / \rho th)] \times 100$$

The mean porosity for the four independently tested specimens in each group were 4.0%, 2.8%, 1.5% and 2.0% for S1, S2, S3 and S4 respectively. Approximate four-specimen mean mass pairs transcribed from laboratory records are available for each composition (air/immersed, g): S1 100.0/61.54; S2 100.0/61.83; S3 100.0/62.41; S4 100.0/62.26. These approximate entries are means of the four-specimen group and should not

 2026 IJLERA – All Right Reserved

be considered as the replicate data set. Thus, the original mean porosities of the four specimens can not be calculated independently from the given pairs and no standard deviations for the porosities are given.

3.5 SEM Analysis

A JEOL JSM-6510LV scanning electron microscope (SEM) was used for microstructural examination, and local elemental characterization was done by energy-dispersive X-ray spectroscopy (EDS). The samples were mechanically polished and chemically etched in Keller reagent for 5 s prior to examination. The microstructural morphology of the recycled aluminum specimens was studied using scanning electron microscopy (SEM) and the energy-dispersive X-ray spectroscopy (EDS) was used for obtaining elemental information in the local area. But the observation of the SEM/EDS cannot prove the presence of a particular crystal phase like Mg_2Si or Al_2Cu. In addition, quantitative grain refinement was not found, since the grain-size was not measured.They cannot give information on the determination of crystalline phases or quantitative determination of grain refinement by themselves. X-ray diffraction and quantitative grain-size analysis were not carried out.

4. Results and Discussion

4.1 Mechanical and Microstructural Behavior

The mechanical properties of the 4 alloy compositions that were modified together (Table 4) were different. Hardness increased from 65 HV0.5 (S1) to 82 HV0.5 (S3), while UTS increased from 110 to 160 MPa; both values decreased at S4 (78 HV0.5 and 150 MPa). The differences seen are due to the alloy chemistry changes and not due to alloy Mg or Cu effect. It is not possible to calculate individual contributions of the elements and synergy due to variation in Mn[5].

For the UTS, the values were raised from S1 (110 MPa) to S3 (160 MPa) and then slightly reduced to S4 (150 MPa). On the other hand, elongation gradually decreased from 12% (S1) to 6% (S4), reflecting a balance between strength and ductility[6]. These changes correlate with changes in the overall composition of the alloy and do not reflect effects of Mg or Cu per se. Elongation has been gradually reduced from S1 to S4 to 12% to 6% respectively which is probably related to increased resistance to plastic deformation and microstructural heterogenecity [2,11]. The other compositions investigated also showed an improvement in strength in all properties, but S3 showed an improved strength/ductility combination.

At 200°C under a constant 2.5 kN tensile load (50 MPa initial nominal stress), software-reported creep rates decreased from 5.2×10^{-6} s^{-1} for S1 to 2.5×10^{-6} s^{-1} for S3, before increasing to 3.0×10^{-6} s^{-1} for S4. Average strain–time curve data presented are average of four specimens each of the four compositions. Since no software rate-fitting window or individual specimen record was available, and so the reported rates are considered to be comparative statistics and not independent steady state slopes, they may not be compared directly with other rates.

The reported mean porosity decreased from 4.0% (S1) to 1.5% (S3), then increased to 2.0% (S4). The measurements were taken for four specimens for each composition and there is an approximate arithmetic cross check in the laboratory, with mass records. However, full set of specimen level mass measurement is not available to independently test reported group means. There is a possibility of influence of oxide entrainment, dissolved hydrogen and microstructural constituents on the porosity which could not be isolated during the experiments. The removal of floating slag and surface oxides by hand is not equivalent to degassing the melt as the dissolved hydrogen in the molten aluminum is not removed.

The SEM/EDS images showed elemental variations and some localised areas of higher concentration of elements Mg and Cu. But EDX is not suitable for determining the occurrence of specific phases, like Mg_2Si and Al_2Cu.The local EDS results for S1 differed from the bulk chemical composition measured by OES, particularly for Si and Mn. The composition of the measured OES are listed in Table 2.

The composition with lowest mean porosity (1.5%), highest ultimate tensile strength (160 MPa) and highest Vickers hardness (82 HV0.5) among the investigated compositions was composition S3. Moreover, software reported the lowest creep rate of 2.5×10^{-6} s^{-1} in S3. Its elongation, however, dropped to 8% as compared with S1 which was 12%, showing a balance between mechanical strength and ductility. As a result, within the range of compositions studied the best combination of evaluated properties was achieved with S3. The optimum performance of S3 is therefore only for the properties investigated and only for the composition range investigated, and no claim of a universal optimum is made.

 2026 IJLERA – All Right Reserved

Table 4: Summary of experimental results for recycled aluminum alloys S1–S4.

Sample	Hardness (HV0.5)	**Porosity (%)**	**UTS (MPa)**	**Elongation (%)**	Software creep rate ($\times 10^{-6}$ s^{-1})
S1	65 ± 1.1	4.0	110 ± 3	12 ± 0.5	5.2
S2	72 ± 1.3	2.8	135 ± 4	10 ± 0.4	3.8
S3	82 ± 1.5	1.5	160 ± 5	8 ± 0.3	2.5
S4	78 ± 1.4	2.0	150 ± 4	6 ± 0.4	3.0

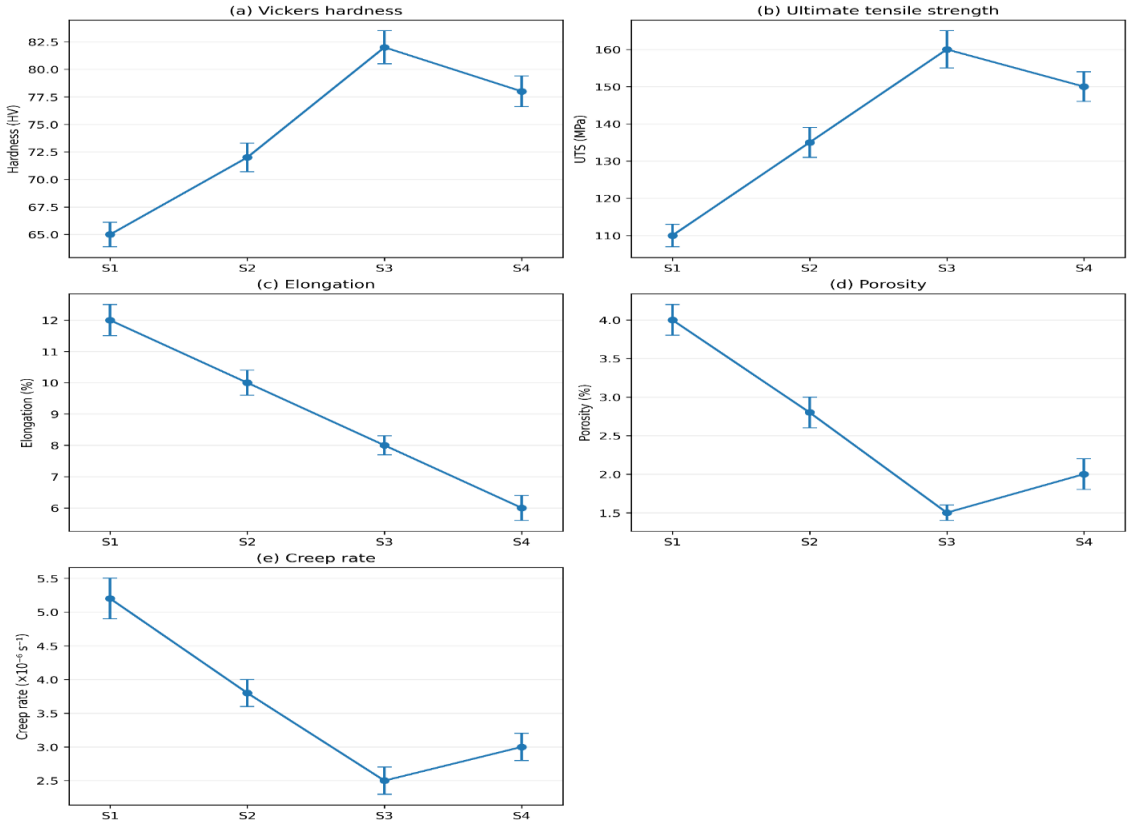


Fig. 3. Experimental properties of the recycled aluminum castings S1-S4 compared: (a) Vickers hardness; (b) ultimate tensile strength (UTS); (c) elongation; (d) mean porosity; and (e) software-reported creep rate. Porosity and creep rate data are not shown with error bars due to the fact that the data records needed to determine the standard deviation of these measurements were not available.

4.2 SEM & EDAX Results

SEM observations showed that there are differences in the microstructural regions studied. Local elemental data, such as the Mg and Cu signals, were provided by EDS. But SEM – EDS alone cannot be used to confirm the presence of certain crystalline phases like Mg_2Si or Al_2Cu. The changes in the mechanical properties all three elements (Mg, Cu and Mn) undergo at the same time makes it difficult to assign the observed mechanical changes to any single alloying element. Claims for quantitative grain refinement are not made.

EDS does not give an overall bulk alloy elemental composition and should not be used to make this determination. Hence, discrepancies between local EDS and bulk OES results can be due to differences in the area analyzed, as well as to differences between two techniques. The differences between the local EDS values of the S1 and the bulk OES values are an example of the effect from the analysis area selected. Table 2 shows that the bulk chemical composition was reported by OES. It is necessary to perform further characterization to confirm the phases and the variations of grain-size, which were not done in this study.

 2026 IJLERA – All Right Reserved

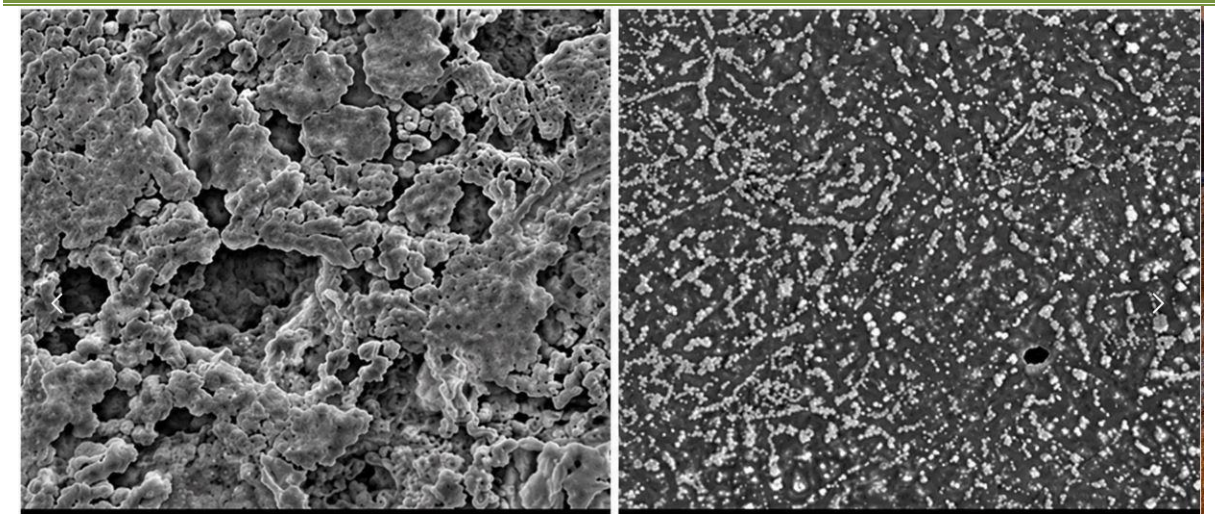


Fig. 4. SEM micrographs of (a) S1, recycled aluminum without additions, and (b) S3, with nominal additions of 2 wt.% Mg and 1 wt.% Cu. The images show differences in observed microstructural morphology; phase identity and grain refinement were not determined.

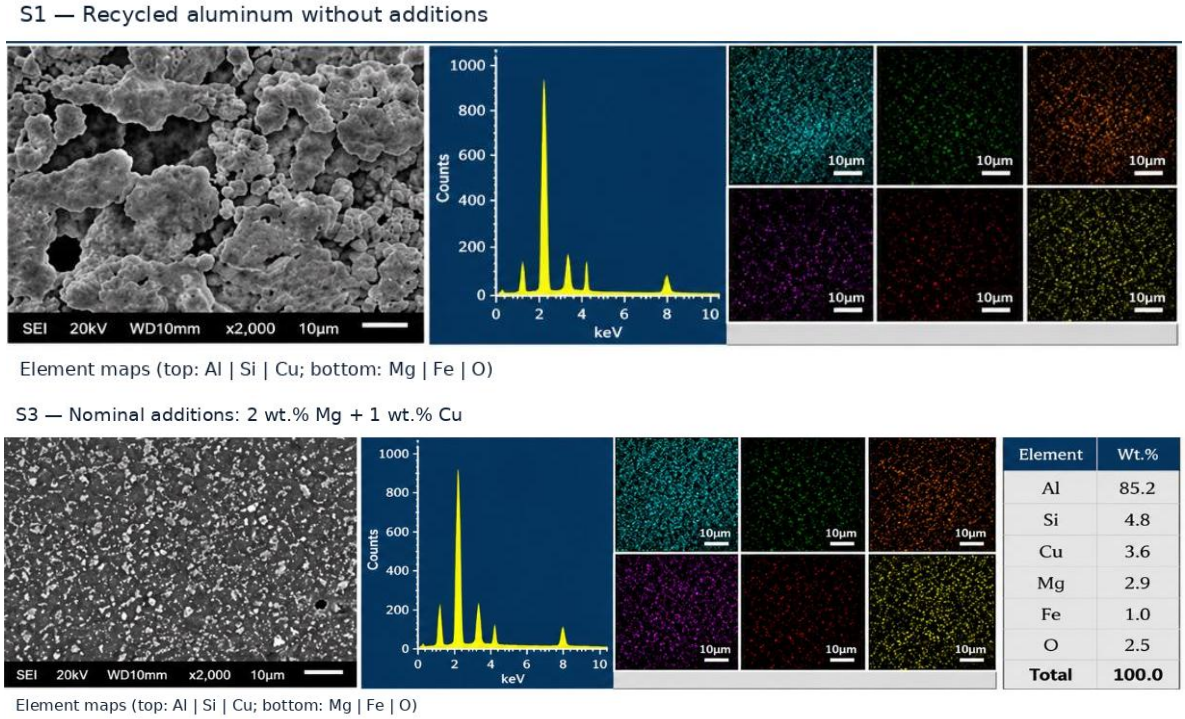


Fig. 5. SEM micrographs, EDS spectra, and elemental distribution maps of (a) S1 and (b) S3. The maps show localized Al, Si, Cu, Mg, Fe, and O signals. EDS does not independently identify Mg_2Si, Al_2Cu, or other crystalline phases.

5. Conclusion

This investigation compared four as-cast recycled aluminum compositions produced from post-consumer beverage cans using the same gravity-casting procedure. The study evaluated how changes in the combined alloy composition were associated with tensile behavior, Vickers hardness, tensile creep response, measured porosity, and selected microstructural features. The experimental comparisons provide composition-specific evidence for the processing conditions investigated, rather than establishing the separate causal effects of individual alloying elements.

Among the investigated compositions, S3, prepared with nominal additions of 2 wt.% Mg and 1 wt.% Cu, exhibited the highest reported ultimate tensile strength (160 MPa) and Vickers hardness (82 HV0.5). The corresponding values for the unmodified recycled aluminum composition S1 were 110 MPa and 65 HV0.5. S4

 2026 IJLERA – All Right Reserved

showed slightly lower strength and hardness than S3, at 150 MPa and 78 HV0.5, respectively. These findings indicate that increasing the nominal alloying additions throughout the entire investigated range did not produce a continuous improvement in these two properties.

The improvement in strength was accompanied by a reduction in ductility. Reported elongation decreased from 12% for S1 to 10% for S2, 8% for S3, and 6% for S4. Accordingly, the selection of a composition for engineering use must consider the required balance between resistance to tensile loading and capacity for plastic deformation. The present data do not support identifying a universally superior alloy for all loading conditions or service environments.

Under the specified creep-test conditions of 200°C, a constant tensile load of 2.5 kN, and a test duration of 3600 s, S3 exhibited the lowest software-reported creep rate (2.5×10^{-6} s^{-1}), compared with 5.2×10^{-6} s^{-1} for S1. The mean recorded porosity was also lowest for S3 (1.5%), compared with 4.0% for S1. Nevertheless, the absence of complete specimen-level density measurements, individual creep traces, and the software rate-fitting interval prevents independent verification of uncertainty for these particular outcomes. The reported creep rates should therefore be interpreted as descriptive comparisons under the applied test conditions rather than independently established steady-state creep rates.

SEM observations and local EDS signals revealed differences between the selected microstructural regions of S1 and S3. These observations provide supporting descriptive evidence but cannot establish the identity of crystalline intermetallic phases or demonstrate quantitative grain refinement. Moreover, measured bulk Mg, Cu, and Mn concentrations changed together across the four compositions. Consequently, the observed property differences cannot be attributed uniquely to magnesium, copper, their interaction, or any particular phase without additional controlled experiments.

Within the tested composition range and for the evaluated properties, S3 provided the most favorable measured combination of strength, hardness, porosity, and reported creep response, with a concurrent loss of elongation relative to S1. Potential applications include recycled aluminum cast components for which strength and hardness are priorities, provided that application-specific durability and qualification testing is completed. Future work should include controlled variation of Mg, Cu, and Mn independently, complete replicate-level density and creep records, melt-treatment comparisons, X-ray diffraction for phase identification, quantitative grain-size analysis, and evaluation under additional temperatures and loading durations.

References

[1]. Samuel, F. H., Samuel, A. M., Doty, H. W., & Valtierra, S. (2017). On porosity formation in Al–Si–Cu cast alloys. In Light Metals 2017 (pp. 243-255). Cham: Springer International Publishing.

[2]. Abdelaziz, M. H., Elgallad, E. M., Doty, H. W., & Samuel, F. H. (2021). Strengthening precipitates and mechanical performance of Al–Si–Cu–Mg cast alloys containing transition elements. Materials Science and Engineering: A, 820, 141497.

[3]. Caceres, C. H., Davidson, C. J., Griffiths, J. R., & Wang, Q. G. (1999). The effect of Mg on the microstructure and mechanical properties of Al–Si–Mg casting alloys. Metallurgical and Materials Transactions A, 30, 2611–2618.

[4]. Tiryakioğlu, M., Campbell, J., & Alexopoulos, N. D. (2009). On the ductility potential of cast Al–Cu–Mg (206) alloys. Materials Science and Engineering: A, 506(1-2), 23-26.

[5]. Shabestari, S. G. (2004). The effect of iron and manganese on the formation of intermetallic compounds in aluminum–silicon alloys. Materials Science and Engineering A, 383, 289–298.

[6]. Campbell, J. (2006). Entrainment defects. Materials science and technology, 22(2), 127-145.

[7]. Davis, J. R. (1993). Aluminum and Aluminum Alloys. Materials Park, OH: ASM International.

[8]. Mondolfo, L. F. (1976). Aluminum Alloys: Structure and Properties. London: Butterworths.

[9]. Totten, G. E., & MacKenzie, D. S. (2003). Handbook of Aluminum: Alloy Production and Materials Manufacturing. New York: Marcel Dekker.

[10]. Hansen, N. (1977). The effect of grain size and strain on the tensile flow stress of aluminium at room temperature. Acta Metallurgica, 25(8), 863-869.

[11]. Hatch, J. E. (1984). Aluminum: Properties and physical metallurgy: ASM International. Materials Park (OH), 32-6.

[12]. Flemings, M. C. (1974). Solidification Processing. New York: McGraw-Hill.

[13]. Shaker, A. O., Rodhan, Z. K., & Hadi, K. A. (2025). Improving mechanical and physical properties of 6061 Al alloy via nano-aluminum and ceramic reinforcement using gravity casting. Archives of Foundry Engineering, 25, 118–123.

 2026 IJLERA – All Right Reserved

[14]. Kazeem, A., Badarulzaman, N. A., & Ali, W. F. F. W. (2020). Relating fractographic analysis to yield strength of novel X7475 (Al–Zn–Mg–Cu) alloys produced by recycling aluminium beverage cans. Materials Letters, 262, 127067.https://doi.org/10.1016/j.matlet.2019.127067

[15]. Abubakar Kazeem, M. H. Rady, A. J. Amkpa, N. A. Badarulzaman, & W. F. F. Wan Ali. (2019). Preliminary morpho-mechanical investigation of X7475 Al-alloys produced from recycled beverage can. Universal Journal of Mechanical Engineering, 7(6C), 7–14. https://doi.org/10.13189/ujme.2019.071602

[16]. Khamsuk, S., Nakvachiratrakul, C., & Chomsaeng, N. (2023). Investigation and improvement of the properties of recycled aluminum alloy. Journal of Science and Technology Mahasarakham University, 42(5), 166–177.

[17]. Gül, K. A., Sahin, H., & Dispinar, D. (2025). Assessment of Mechanical Behaviors of Sand Cast Al-Mg7-Cu2 Aluminum Alloy in Tilt and Vertical Gravity Casting Conditions. Archives of Foundry Engineering, 25(1), 169–179. https://doi.org/10.24425/afe.2025.153787

[18]. Rajagukguk, K., Suyitno, S., Saptoadi, H., Kusumaningtyas, I. K. I., Arifvianto, B., & Mahardika, M. (2024). Remelting of Aluminum Scrap into Billets Using Direct Chill Casting. Archives of Foundry Engineering, 24(1), 40–49. https://doi.org/10.24425/afe.2024.149250

[19]. Mohamed, A. M. A., Samuel, E., Samuel, A. M., Doty, H. W., Songmene, V., & Samuel, F. H. (2023). Effect of intermetallics and tramp elements on porosity formation and hardness of Al–Si–Mg and Al–Si–Cu–Mg alloys. International Journal of Metalcasting, 17(2), 664–681. https://doi.org/10.1007/s40962-022-00813-w

[20]. Raabe, D., Ponge, D., Uggowitzer, P. J., et al. (2022). Making sustainable aluminum by recycling scrap: The science of “dirty” alloys. Progress in Materials Science, 128, 100947. https://doi.org/10.1016/j.pmatsci.2022.100947.

 2026 IJLERA – All Right Reserved